Vol. **110** (2006) *ACTA PHYSICA POLONICA A* No. 1

Surface Magnetic Anisotropy of Epitaxial $La_{0.7}Mn_{1.3}O_{2.84}$ Thin Films

P. Aleshkevych[a,*], M. Baran[a], V. Dyakonov[a], R. Szymczak[a], H. Szymczak[a], K. Baberschke[b], J. Lindner[b,†] and K. Lenz[b]

[a]Institute of Physics, Polish Academy of Sciences
al. Lotników 32/46, 02-668 Warsaw, Poland
[b]Institute für Experimentalphysik, Freie Universität Berlin
Arnimallee 14, 14195 Berlin, Germany

(Received September 14, 2005; revised version January 30, 2006; in final form May 31, 2006)

A spin-wave resonance technique was used to collect information on elementary magnon excitations in high quality epitaxial $La_{0.7}Mn_{1.3}O_{2.84}$ films prepared by dc-magnetron sputtering. It was found that besides bulk spin-wave modes, the spin-wave resonance spectrum includes also the surface spin waves. The value of spin-wave stiffness constant $D = 156$ meV·Å^2 was found. The values of the surface magnetic anisotropy on both surfaces and their angular dependence were determined. The experimentally found spin-wave resonance spectra were explained based on the surface-inhomogeneity model. The effect of surface anisotropy on the spin-wave excitation conditions in epitaxial $La_{0.7}Mn_{1.3}O_{2.84}$ films was investigated. Spin-wave resonance data give an indirect evidence of periodic charge-ordered stripes formation.

PACS numbers: 76.50.+g, 75.70.–i

1. Introduction

The doped rare-earth manganites $La_{1-x}A_xMnO_{3-\delta}$ (A = Ca, Sr, Ba,...) have attracted a considerable interest in recent years (see for example review pa-

*corresponding author; e-mail: pavloa@ifpan.edu.pl
†present address: Institut für Physik, Universität Duisburg-Essen, Lotharstr. 1, 47048 Duisburg, Germany

pers [1–3]) motivated by the observations of their unusual magnetic and transport properties. A parent compound for these manganites is stoichiometric antiferromagnetic (AFM) $LaMnO_3$, with $T_N = 140$ K [4], containing only Mn^{3+} ions with ferromagnetic (FM) ordering in the (*ab*) Mn–O planes, which, in turn, form the AFM lattice along the *c* axis. The transition to the ferromagnetic state takes place by La ions substitution for divalent alkaline earth ions or by formation of Ls^{3+} cation deficiency [5]. Non-stoichiometric $La_{0.7}Mn_{1.3}O_{2.84}$ is characterized by the presence of vacancies in both cation and anion sublattices that produce the mixed valence states of Mn ions [6]. Such samples are self-doped systems and show a colossal magnetoresistance (CMR) at the manganese content of 1.1–1.3 [7]. A number of experimental data provide evidence (see Ref. [8] and reference therein) in favour of the magnetic phase separation existing in non-stoichiometric manganites. Generally, the inhomogeneities in manganites arise from phase competition between ferromagnetic metallic and charge-ordered insulating phases [9–11] and this fact is frequently involved to explain their unusual magnetic and transport properties. Recently in many papers, mostly theoretical, it is assumed the occurrence of the electronic phase separation in manganites, where the formation of inhomogeneities in the real materials, at a nanometer scale [12], plays a key role. The purpose of this work is to study the magnetic properties, particularly the surface magnetic properties, of non-stoichiometric $La_{0.7}Mn_{1.3}O_{2.84}$ films by means of microwave technique.

The transport properties, electron and nuclear magnetic resonance in these films have been studied earlier [6, 7]. The previously performed magnetization measurements have revealed that the films investigated are ferromagnets ($T_C = 205$ K) with low temperature changes of magnetization satisfactorily described in terms of the spin-waves theory [13]. The preliminary measurements of spin-wave resonance (SWR) have shown that these films are ideal for studying magnetic interactions in manganites using the microwave technique because narrow resonance lines confirm their high-quality and chemical uniformity [14].

There are three experimental techniques for studying magnetic excitations: inelastic neutron scattering, Brillouin scattering, and microwave techniques. Inelastic neutron scattering is inapplicable to thin films. The Brillouin scattering technique could be used for studying thin films but at the present time there are no reports about using this technique in thin films of manganites. However, there are two reports in the literature where Brillouin scattering was used for studying the bulk and surface spin-wave excitations in polycrystalline and single crystals of manganites [15, 16]. A big advantage of the microwave technique consists in fact that it could be applicable for thin or ultra-thin films. There are a few reports concerning SWR in the thin films of manganites. Previously SWR was observed in $La_{0.7}Ba_{0.3}MnO_3$ [17, 18] and La–(Sr,Ca)–Mn–O films [19] apart our previous publications [13, 14, 20]. The observation of the surface spin waves has a special interest in modern physics since resonance lines related to surface spin waves

provide direct information concerning magnetic surfaces. The SWR spectra are extremely sensitive to any changes in magnetic structure of the films and in particular to changes of the magnetic structure on the surfaces of films. It will be shown that the microwave technique can be as valuable as inelastic neutron scattering in studying elementary magnetic excitations. In addition it allows the study of such phenomena as stripe formation and volume or surface magnetic anisotropies.

2. Experiment

The $La_{0.7}Mn_{1.3}O_{2.84}$ films preparation has been described previously in [6, 21]. In brief, the films were deposited onto [001] oriented $LaSrAlO_4$ substrates by on-axis dc-magnetron sputtering with post preparation annealing in an oxygen atmosphere at 700°C for 30 min. The thickness of the layers was estimated to be about 3500 Å. A structural analysis has confirmed that these high quality epitaxial films are oriented along a pseudo-cubic axis [100] and their lattice constant is 3.907 Å.

The SWR experiments have been carried out using the X-band spectrometer with a reflection cavity, operating at a fixed frequency of about 9.25 GHz and equipped with a variable temperature flowing gas cryostat.

3. Experimental results and analysis

It was found that the spectrum at the out-of-plane magnetic field geometry reveals a complex structure at temperatures below the Curie temperature. The greatest numbers of resonance peaks were found in a spectrum measured when the static magnetic field is applied perpendicularly to the surfaces of the film. The profile of the spectrum strongly changes with a deviation from the perpendicular configuration. Characteristic examples of SWR spectra recorded at different values of the angle between a normal to the film and a magnetic field $\boldsymbol{H}$ direction (labelled as the angle θ_H further in the text) are shown in Fig. 1. An important feature of the spectra is the presence of a resonance absorption from surface waves. The resonance peaks associated with surface spin waves are labelled as SM in Fig. 1. The spectrum has only one surface mode ($SM1$) in the perpendicular orientation ($\theta_H = 0°$). By increasing θ_H, the intensity of the surface mode grows, and the distance between this mode and the neighbouring mode decreases (see $\theta_H = 5°$). The intensity of the SM continues to increase to $\theta_H = 9°$ when the surface mode's intensity becomes the greatest among all other modes in a spectrum. Next the spectrum exhibits one resonance peak only at $\theta_H = 11°$. At θ_H greater than 11° the spectrum again consists of several peaks and in this situation even two surface modes can be seen ($\theta_H = 15°$).

To properly explain the obtained SWR spectra the surface-inhomogeneity (SI) model [22] was used (see also references in Ref. [22]). This model describes in detail the influence of the bound (or pinning) conditions at the surfaces of the film, which are responsible for the excitation of standing spin waves. Moreover, in

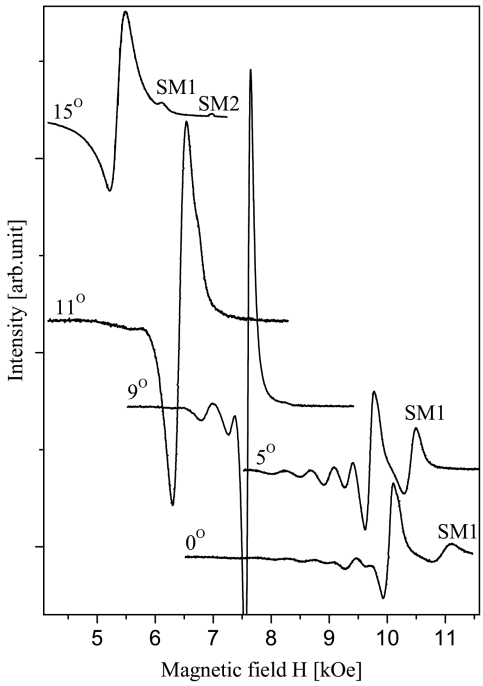

Fig. 1. Examples of SWR spectra recorded for different angles between the normal to the film's surface and magnetic field (θ_H), at $T = 10$ K. The resonance peaks corresponding to surface spin waves are labelled as SM.

frames of the SI model it was possible to explain the excitation of one or two surface spin wave modes. The essence of the SI model relies specifically on the formulated boundary conditions by assuming the existence of a surface anisotropy on each film surface. The boundary conditions were described by a "surface parameter" A given by

$$A = 1 + \frac{E_{\mathrm{S}}(\theta, \phi)}{E_{\mathrm{ex}}}, \tag{1}$$

where E_{S} is the surface anisotropy energy, E_{ex} — the exchange energy, φ — the azimuthal angle between $\boldsymbol{M}$ component in-plane of the film and the $\langle 100 \rangle$ axis, and θ is the polar angle between $\boldsymbol{M}$ and [001] axis (film normal). If there is no surface anisotropy ($E_{\mathrm{S}} = 0$), $A = 1$, and there is no difference between spins on the surface and inside the film. If $E_{\mathrm{S}} > 0$, $A > 1$ and spins on the appropriate surface have a greater energy than the one of the internal spins. $E_{\mathrm{S}} > 0$ is a necessary condition of excitation for the surface wave. In general, each of the film's two surfaces can be characterized by its own surface anisotropy; therefore two surface waves can be excited.

Within the SI model the existence of only one surface (acoustic) wave at the perpendicular orientation is possible in situation when the surface anisotropy

energy of the film has different values at both surfaces. This situation could be expected in these films, since one of the surfaces is in direct contact to the substrate, while another surface can be treated as completely free. The appearance of only one surface wave testifies that on one of the surfaces, the surface anisotropy $E_S > 0$ (it is on the free surface as it will be shown later), while on another surface (interface) the spins are pinned (i.e. $E_S < 0$). In other words in the given film the asymmetric boundary conditions are realized. Therefore this film should be characterized by two different surface parameters: A_f and A_S for free surface and interface, respectively. As for volume spin waves, this asymmetry in the boundary conditions makes it possible to excite the asymmetrical spin waves in the spectrum in addition to the symmetrical modes. This fact is in contrast to a majority of reports concerning SWR, where symmetrical boundary conditions are usually assumed and therefore the SWR spectrum is confined to the symmetrical waves only.

In fact, the analysis of the SWR spectra is more complicated because the surface anisotropy is assumed to depend on the directions of the magnetization in the sample and this dependence for the surface parameter can be expressed by the following series expansion in spherical harmonics [23]:

$$A(\theta, \phi) = \sum_{l=0}^{\infty} \sum_{m=-l}^{l} A_{lm} Y_{lm}(\theta, \phi), \tag{2}$$

where θ and φ are the same angles as in Eq. (1).

The existence of the angular dependence of the surface parameters on each surface allows an experimental realization of various combinations of asymmetric boundary conditions by simple rotation of a sample in an external magnetic field. One of these combinations is the prediction of a critical angle where the SWR spectrum is reduced to the single resonance peak ($\theta_H = 11°$). In this case the boundary conditions on both surfaces become equal ($A_f = A_S = 1$). Configurations where SWR spectrum shows two surface waves are possible only if the spins are unpinned on both surfaces ($A_f > 1$, $A_S > 1$). Another example of configuration effects is the case when the value of A_S on the interface passes through 1 at the rotation of the film in the magnetic field. Meanwhile, the free surface parameter A_f remains above 1, being equal to 1.007, 1.005, 1.003 for $\theta_H = 5°$, $7°$, and $9°$, respectively. The resonance lines integral intensity vs. mode number is shown in Fig. 2 for three values of θ_H. At $\theta_H = 7°$, when the effect of the surface anisotropy on the interface disappears ($A_S = 1$), the intensity of the symmetric waves (peaks with even numbers) as well as asymmetric ones (peaks with odd numbers) form a monotonous line. At angles $\theta_H < 7°$, the line connecting the intensity of even peaks lies higher than that connecting odd peaks, and at $\theta_H > 7°$ — vice versa.

The important point for a correct interpretation of SWR spectra is the analysis of the intensity of the resonance peaks. If the spectrum consists of at least three peaks for an arbitrary chosen configuration of magnetization (described by the an-

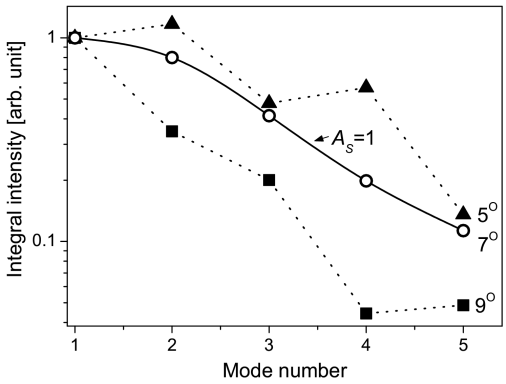

Fig. 2. The resonance lines integral intensity vs. mode number for several values of θ_H. At $\theta_H = 7^\circ$ $A_\mathrm{S} = 1$. The figure illustrates the effect of mutual over-passing of the intensity envelopes for the two kinds of peaks (even and odd).

gles θ and ϕ) the value of each surface parameter can be calculated numerically from the resonance peak relative intensities, recorded at that configuration [22]. In calculations described as the asymmetrical pinning (RIAP) method [22], A_f and A_S are free parameters and are used to determine the theoretical values of the intensities. An example of the result of such calculations for the spectrum in the perpendicular orientation is shown in Fig. 3 and the best agreement between calculated and experimental values was found for $A_\mathrm{f} = 1.012$ and $A_\mathrm{S} = 0.960$.

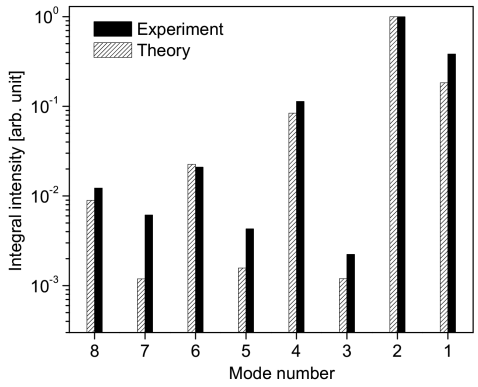

Fig. 3. The resonance line intensity vs. mode number for resonance spectrum recorded at $T = 10$ K for the perpendicular orientation (solid columns) and theoretical values of intensity calculated for $A_\mathrm{f} = 1.012$ and $A_\mathrm{S} = 0.960$ using the SI model (dashed columns).

Using the RIAP method, the angular dependence of surface parameters at a temperature 10 K was calculated and the results of the calculation are presented in Fig. 4a. There are shown: the values of surface parameters on the left vertical axis and the equivalent values of surface anisotropy energy on the right vertical axis.

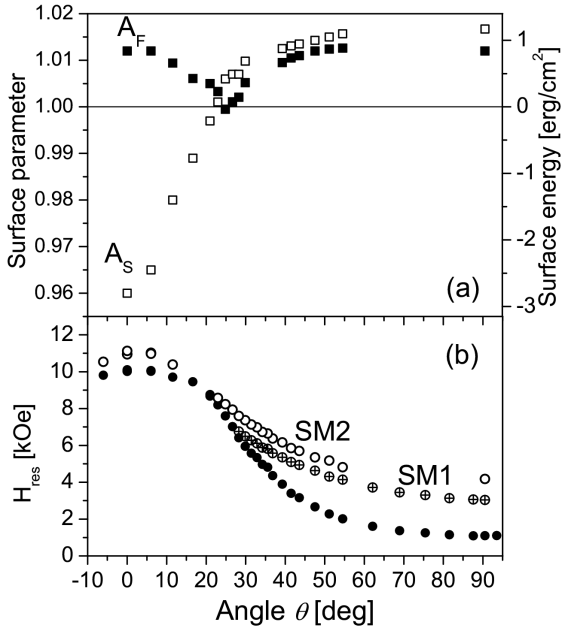

Fig. 4. (a) The angular dependence of the surface parameters for the free ($A_{\rm f}$) surface and the interface ($A_{\rm S}$) calculated for 10 K. The scale on the right hand side gives the surface anisotropy energies that are proportional to the surface parameters. (b) The angular dependence of the resonance field for two surface waves and the first volume spin wave.

For a better presentation the angular dependence of the resonance field for two surface modes and the first volume mode is shown in Fig. 4b. The magnetic field rotates in plane containing both [001] and [110] directions. The value of $4\pi M_{\rm eff}$ calculated from $H_{\rm res}(\theta)$, shown in Fig. 4b, is found to be 7165 Oe ($M_{\rm eff} \approx 570$ Oe). It should be noted that the angle θ was used instead of θ_H. The vector $\boldsymbol{M}$ is not parallel to $\boldsymbol{H}$, when an applied magnetic field is comparable with a magnetic anisotropy and demagnetization fields. The direction θ of $\boldsymbol{M}$ with respect to the normal of the film was found from the following equilibrium condition:

$$2H\sin(\theta - \theta_H) = H_{\rm eff}\sin(2\theta). \tag{3}$$

where H is the applied external magnetic field, $H_{\rm eff}$ is the effective field including the bulk anisotropy field and demagnetization fields. In our case $H_{\rm eff}$ is estimated to be equal to 6.8 kOe at $T = 10$ K.

In Fig. 4 one can see that two surface modes appear, when both surface parameters are greater than 1, whereas only one surface mode appears when only $A_{\rm f} > 1$. With these surface parameters, the values of the wave vectors for the volume spin waves were calculated, by solving the following characteristic equation [22]:

$$\mathrm{tg}(Lk) = \frac{(A_\mathrm{f}A_\mathrm{S} - 1)\sin(ka)}{(A_\mathrm{f}A_\mathrm{S} + 1)\cos(ka) - (A_\mathrm{f} + A_\mathrm{S})}, \tag{4}$$

where k is the wave vector, L — the thickness of the film, and a — the lattice constant. Wave vectors of surface waves have pure imaginary values and their modules are calculated by solving the same Eq. (4), where hyperbolic functions are substituted for the trigonometric functions.

It is known from the theory of spin waves that in ferromagnets the energy of spin waves $E = Dk^2$ for $k \to 0$, where D is the spin-waves stiffness. In turn, the position of the resonance peaks is proportional to the energy of the spin waves according to the well-known Kittel's resonance condition [24]:

$$\frac{\omega}{\gamma} = H_\mathrm{res} - 4\pi M_\mathrm{S} + H_\mathrm{a} + Dk^2, \tag{5}$$

where H_res is the resonance field, ω — the resonance frequency, M_S — the saturation magnetization, H_a — the anisotropy field and γ — the spectroscopic splitting ratio. Equation (5) is fulfilled for $\boldsymbol{H}$ perpendicular to the film plane. In the case of perfect pinning of the surface spins the spin-wave vector is equal to $\pi na/L$, where n is the integer numbers and, as it follows from Eq. (5), the dependence of $(H_0 - H_n)$ as a function of $2n+1$ should be linear. However, the case of the perfect pinning is rather ideal, because of surface anisotropy according to the perfect pinning should have a negative infinite value. In our case, the surface spins are partly pinned and the appropriate surface anisotropy is finite. If spin-wave vectors k are the solutions of the characteristic Eq. (4), $k1$ — the spin-wave vector of the first volume spin wave and H_k — the resonance field corresponding to the spin-wave vector k, then the dependence of $(H_{k1} - H_k)$ as a function of $2(kL/\pi a)+1$ should be linear. This dependence for a spectrum in the perpendicular orientation is shown in Fig. 5. The resonance field of surface mode is not shown, because its spin-wave vector has a pure imaginary value. From the slope of the solid line, which is the

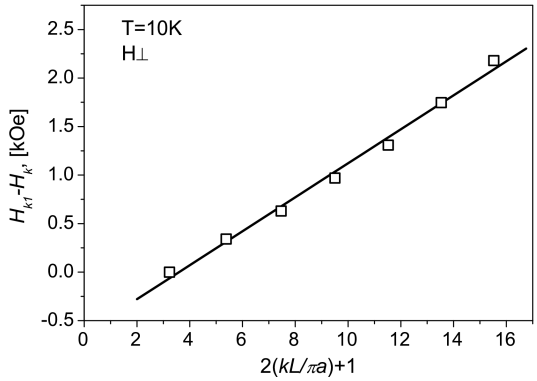

Fig. 5. The difference between resonance field of first volume spin wave and other $(H_{k1} - H_k)$ as a function of $2(kL/\pi a)+1$. Let us note that the values of k are normalized to the lattice constant and therefore are dimensionless.

best approximation to the experimental data, a value of $D = 156$ meV $\cdot$ Å^2 was found. In this case D is the average bulk exchange constant. This value agrees with the value determined from the analysis of the saturation magnetization as a function of temperature [13].

The results described above are related to the wave excitations in the low temperature region, where ferromagnets are characterized by a high degree of spin ordering. In this analysis the magnon–magnon interactions were neglected. But the SWR spectra change with increasing temperature. It means that the surface anisotropy changes with temperature similarly to the volume magnetic anisotropy. Figure 6 shows the integral intensity of spin wave modes vs. mode numbers for

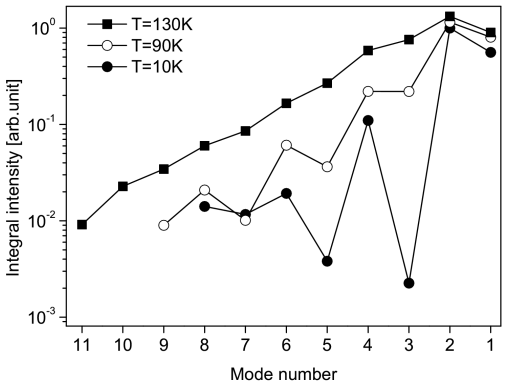

Fig. 6. The resonance peak intensity vs. mode number for the three temperatures (10 K, 90 K, 130 K).

spectra recorded in the perpendicular configuration at three different temperatures ($T = 10$ K, 90 K, and 130 K). At 10 K the intensity of the peaks for even and odd peaks is highly nonmonotonic because of the large asymmetry of the surface anisotropies. By performing the numerical calculations in that way as it was done for the spectrum at $T = 10$ K (see Fig. 3), the following values of the surface parameters were obtained: $A_{\mathrm{f}} = 1.006$, $A_{\mathrm{S}} = 0.96$ for $T = 90$ K and $A_{\mathrm{f}} = 1.002$, $A_{\mathrm{S}} = 0.96$ for $T = 130$ K. As the temperature increases, the interface anisotropy remains unchanged, but the free surface anisotropy decreases and consequently the asymmetry decreases resulting in a more monotonous intensity dependence.

The well-resolved splitting of the resonance lines (into two lines) appears at $T > 150$ K, however it is also possible to recognize the doublet structure of resonance lines at lower temperatures. This splitting grows with increasing temperature. A typical example of such a spectrum recorded at 155 K is shown in Fig. 7. The inset in Fig. 7 shows the splitting between adjacent resonance lines within the doublet vs. T. It is seen that the splitting monotonously grows up to the Curie temperature $T_{\mathrm{C}} = 205$ K. This "doublet structure" of SWR spectrum can be comprehensively explained within the framework of the SI model and

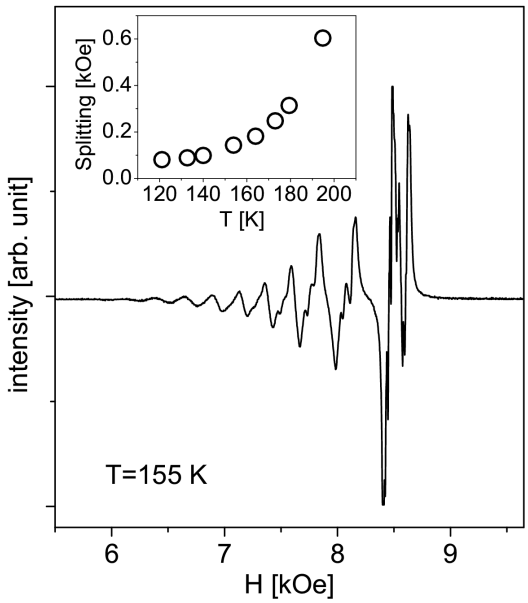

Fig. 7. An illustration of the "doublet" structure of the SWR spectrum recorded in the perpendicular orientation at $T = 155$ K. The inset shows the distance between adjacent resonance lines within the doublet vs. T.

points to forming two magnetic sublattices (or stripes) on the surface [20]. The SWR does not answer the question: what makes these magnetic sublattices, but points that the surface anisotropy varies on one of the surfaces and this variation is periodical. The application of this technique for observation of the stripes was possible because of the specific influence of the periodic boundary conditions on SWR spectra in the periodically magnetic inhomogeneous materials.

It is known [5, 25] that in manganites an excess of oxygen ($LaMnO_{3+d}$) as well as in $La_{0.7}Mn_{1.3}O_{2.84}$ [6] presented in this study the appearance of Mn ions in mixed valence states is a result of charge compensation caused by the enhanced defect structure. In general, in this crystal structure there exist vacancies in both the cation and anion sublattices. Moreover, those studies showed that the defect chemistry can be described with a cluster model, where cation and anion vacancies may not only be randomly distributed but also form more complex defects — mesoscopic cluster-type inhomogeneities [6, 26, 27]. The surface chemical segregation phenomena were observed in rare-earth doped manganites [28–31]. It was found that the surface composition dramatically differs from its bulk counterpart, which strongly affects the magnetic properties of surface. Furthermore, it was pointed in [28] that the surface segregation should be expected in metal oxides of ionic nature because of the existence of a space-charge layer in the near surface region, providing a strong chemical potential, which drives surface segregation.

Choi et al. [30] found that in Ca-doped manganites there is preferential Ca segregation to the surface against random distribution. It was also found that a simple description of the Mn valence in terms of a mixed Mn^{3+}/Mn^{4+} state may be not valid at the surface because of the presence of Mn^{2+} ions [31].

The probable ordering of oxygen vacancies in the self-doped $La_{0.7}Mn_{1.3}O_{2.84}$ is in favour of suggested stripe formation by the Mn ions with different valence. Any type of oxygen vacancies (as well as paramagnetic Mn^{2+}) cannot directly affect the resonance lines. However, oxygen vacancies that would assist the electronic ordering of the separation of the Mn ions could also assist charge ordering.

In our films the Mn^{3+}/Mn^{4+} ratio is equal to 2:1, it is assumed that the stripe formation has a period of three lattice constant $= 3a$. SWR has no splitting at low temperature where exchange interaction length $> 3a$ and two magnetic sublattices are effectively averaged [20]. The splitting of the SWR lines starts at that temperatures when exchange interaction length will decrease so much as it becomes comparable with or less than a stripe period.

4. Discussion

Generally, the information on the surface magnetic anisotropy allows for deeper insight into the microscopic nature of surface magnetic interactions. However in our case, due to the complexity of calculations, it was difficult to achieve the full quantitative agreement with the experiment. For this reason the interpretation presented below is proposed to explain *qualitatively* the angular dependence of the surface anisotropy.

The first nonzero terms in the sum (2) are the Legendre polynomials P_0, P_2, P_4, therefore the surface parameter will be assumed to have the following form:

$$A = a_0 + \frac{a_2}{2}\left(3\cos^2\theta - 1\right) + \frac{a_4}{8}\left(35\cos^4\theta - 30\cos^2\theta + 3\right), \tag{6}$$

where the microscopic parameters a_0, a_2, a_4 are responsible for the strength of the exchange, dipolar magnetic, and quadrupolar interactions, respectively. A single-ion mechanism via spin–orbit interaction can also give rise to the surface anisotropy producing the $\cos^4\theta$ dependence in cubic crystals. At relatively high temperatures where charges are well localized and SWR spectra are showing the doublet structure, Mn^{3+} and Mn^{4+} ions can be characterized by their own surface parameters, namely, A_{f1} and A_{f2}. In this case the splitting between lines within the doublet will be maximal (see the inset in Fig. 7). The $3d^3$ electronic configuration of Mn^{4+} is nearly spherically symmetric while Mn^{3+} is highly asymmetric because of the Jahn–Teller distortion associated with the removal of the two-fold orbital degeneracy of the e_g orbitals. This suggests that the Mn^{4+} is the only candidate that can be responsible for the $\cos^4\theta$ dependence in the anisotropy energy while Mn^{3+} may be responsible for the $\cos^2\theta$ (although a contribution of Mn^{3+} ions to cubic anisotropy cannot be neglected). Upon lowering the temperature, the charge order is "melted" due to the double exchange interaction averaging the different

anisotropies. In this case the free surface will be characterized by one average value $A_{\rm f} = (1-\alpha)A_{\rm f1} + \alpha A_{\rm f2}$ (where α is the amount of Mn^{4+}) with the complex angular dependence given by Eq. (6) while the splitting between lines within the doublet will tend to disappear. On the opposite side of the film one should take into account the fact that there is a slight mismatch of lattice constants of the film (3.907 Å) and the substrate (3.764 Å in *ab*-plane). Therefore one may suppose that on this interface a periodic magnetic inhomogeneity cannot exist and over a wide temperature range the interface will be characterized by some average surface parameter $A_{\rm S}$ described by the $\cos^2\theta$ dependence resulting from the uniaxial dipolar interactions. The small value of the critical angle ($\theta = 27^\circ$) points

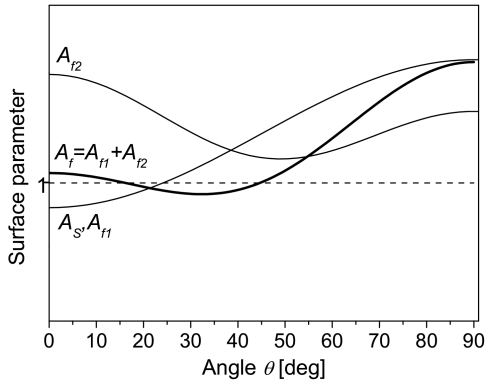

Fig. 8. The angular dependence of the theoretically calculated surface parameters as explained in the text.

indirectly on relatively large contribution of the isotropic term in both surface anisotropies. Therefore the experimental dependence of the surface parameter can be qualitatively reproduced assuming that $A_{\rm f1}$ and $A_{\rm S}$ are proportional to $\cos^2\theta$ while $A_{\rm f2} \sim \cos^4\theta$ (appropriate dependences are shown in Fig. 8).

5. Conclusion

The $La_{0.7}Mn_{1.3}O_{2.84}$ films were studied by the microwave technique. Different configurational effects were observed in the SWR spectrum as a result of the formation of specific surface anisotropies on both surfaces of the film. The analysis of these modes has delivered information concerning the surface anisotropy in manganite films. The evidence of stripe formation of charge ordered magnetic ions was also obtained from the analysis of the SWR spectra.

Acknowledgments

The authors are grateful to Prof. H. Puszkarski for valuable discussions. The work was partially supported by the State Committee for Scientific Research under contract 1 P03B 025 26.

References

[1] A.P. Ramirez, *J. Phys., Condens. Matter* **9**, 8171 (1997).

[2] J.M.D. Coey, M. Viret, S. Molnar, *Adv. Phys.* **48**, 167 (1999).

[3] J.B. Goodenough, in: *Handbook on the Physics and Chemistry of Rare Earths*, Ed. K.A. Gschneidner, Elsevier Science B.V., Vol. 33, Amsterdam 2003, p. 249.

[4] E.O. Wollan, W.C. Koehler, *Phys. Rev.* **100**, 545 (1955).

[5] J.A.M. Roosmalen, E.H.P. Cordfunke, R.B. Helmholdt, H.W. Zandbergen, *J. Solid State Chem.* **110**, 100 (1994).

[6] V.N. Krivoruchko, S.I. Khartsev, A.D. Prokhorov, V.I. Kamenev, R. Szymczak, M. Baran, M. Berkowski, *J. Magn. Magn. Mater.* **207**, 168 (1999).

[7] V.P. Pashchenko, S.I. Khartsev, O.P. Cherenkov, A.A. Shemyakov, Z.A. Samoilenko, A.D. Loiko, V.I. Kamenev, *Inorg. Mater.* **35**, 1294 (1999).

[8] I.O. Troyanchuk, V.A. Khomchenko, A.N. Chobot, H. Szymczak, *J. Phys., Condens. Matter* **15**, 6005 (2003).

[9] E.L. Nagaev, *Usp. Fiz. Nauk* **166**, 833 (1966).

[10] E. Dagotto, T. Hotta, A. Moreo, *Phys. Rep.* **344**, 1 (2001).

[11] L.P. Lev, P. Gor'kov, V.Z. Kresin, *Phys. Rep.* **400**, 149 (2004).

[12] E. Dagotto, A. Moreo, *J. Magn. Magn. Mater.* **226-230**, 763 (2001).

[13] P. Aleshkevych, J. Lindner, K. Baberschke, V. Dyakonov, H. Szymczak, R. Szymczak, *Phys. Status Solidi A* **196**, 93 (2003).

[14] V. Dyakonov, A. Prokhorov, V. Shapovalov, V. Krivoruchko, V. Paschenko, E. Zubov, V. Mikhailov, P. Aleshkevych, M. Berkowski, S. Piechota, H. Szymczak, *J. Phys., Condens. Matter* **13**, 4049 (2001).

[15] P. Murugavel, C. Narayana, A.K. Sood, S. Parashar, A.R. Raju, C.N.R. Rao, *Europhys. Lett.* **52**, 461 (2000).

[16] C. Narayana, *J. Indian Inst. Sci.* **82**, 103 (2002).

[17] S.E. Lofland, S.M. Bhagat, C. Kwon, M.C. Robson, R. Ramesh, R.P. Sharma, T. Venkatesan, *Phys. Lett. A* **209**, 246 (1995).

[18] M.C. Robson, C. Kwon, K.-C. Kim, R.P. Sharma, T. Venkatesan, S.E. Lofland, S.M. Bhagat, R. Ramesh, M. Dominguez, S.D. Tyagi, *J. Appl. Phys.* **80**, 2334 (1996).

[19] J. Yin, Y.X. Sui, J.H. Du, Y.X. Zhang, X.Y. Liu, Z.G. Liu, *Phys. Status Solidi A* **174**, 499 (1998).

[20] P. Aleshkevych, M. Baran, H. Szymczak, *Acta Phys. Pol. A* **106**, 593 (2004).

[21] V.N. Krivoruchko, S.I. Khartsev, *Low Temp. Phys.* **24**, 803 (1998).

[22] H. Puszkarski, *Prog. Surf. Sci.* **9**, 191 (1979).

[23] H. Puszkarski, *Solid State Commun.* **22**, 563 (1977).

[24] C. Kittel, *Phys. Rev.* **110**, 1295 (1958).

[25] J.F. Mitchell, D.N. Argyriou, C.D. Potter, D.G. Hinks, J.D. Jorgensen, S.D. Bader, *Phys. Rev. B* **54**, 6172 (1996).

[26] W.-N. Wang, Z.-S. Jiang, Y.-W. Du, *J. Appl. Phys.* **78**, 6679 (1995).

[27] L.J. Maksymowicz, D. Sendorek, *J. Magn. Magn. Mater.* **37**, 177 (1983).

[28] H. Dulli, P.A. Dowben, S.-H. Liou, E.W. Plummer, *Phys. Rev. B* **62**, R14629 (2000).

[29] J.-H. Park, E. Vescovo, H.-J. Kim, C. Kwon, R. Ramesh, T. Venkatesan, *Phys. Rev. Lett.* **81**, 1953 (1998).

[30] J. Choi, J. Zhang, S.-H. Liou, P.A. Dowben, E.W. Plummer, *Phys. Rev. B* **59**, 13453 (1999).

[31] M.P. de Jong, I. Bergenti, V.A. Dediu, M. Fahlman, M. Marsi, C. Taliani, *Phys. Rev. B* **71**, 014434 (2005).